Eur. Phys. J. B **42**, 271–277 (2004)
DOI: 10.1140/epjb/e2004-00379-2

THE EUROPEAN PHYSICAL JOURNAL B

Entropy production in the cyclic lattice Lotka-Volterra model

C. Anteneodo[a]

Centro Brasileiro de Pesquisas Físicas, Rua Dr. Xavier Sigaud 150, 22290-180 RJ, Rio de Janeiro, Brazil
and
Departamento de Física, Pontifícia Universidade Católica do Rio de Janeiro, CP 38071, 22452-970 RJ, Rio de Janeiro, Brazil

Received 16 July 2004 / Received in final form 8 October 2004
Published online 14 December 2004 –

Abstract. The cyclic Lotka-Volterra model in a D-dimensional regular lattice is considered. Entropy production of its "nucleus growth" mode is investigated by analyzing the time evolution of the family of entropies $S_q = (1 - \sum_i p_i^q)/(q-1)$, with $q \in \mathbb{R}$. This family contains as particular case ($q = 1$) the usual entropic form $S_1 = -\sum_i p_i \ln p_i$. The rate of growth of the entropy S_q, for some $q \neq 1$, is expected to provide non-trivial information about certain complex systems. For the system here considered, it is shown, both numerically and by means of analytical considerations, that a linear increase of entropy with time, meaning finite asymptotic entropy rate, is achieved for the entropic index $q_c = 1 - 1/D$, as previously conjectured in the literature. However, although $q_c \neq 1$, this relation can be explained in terms of very simple features not directly connected to the complexity of the dynamics. The relation between the characteristic entropic index and lattice dimensionality is shown to be a consequence of the fact that the system soon approaches a steady regime where the nucleus radius grows linearly with time.

PACS. 05.10.Ln Monte Carlo methods – 05.65.+b Self-organized systems – 05.45.-a Nonlinear dynamics and nonlinear dynamical systems

1 Introduction

Over one decade ago, Tsallis proposed an entropic form as a starting point for a possible generalization of Boltzmann-Gibbs statistics [1] (see also [2] for a review on the subject). The generalized entropy has the form

$$S_q = k\frac{1 - \int \mathrm{d}x\,[\rho(x)]^q}{q-1}, \qquad \text{with } q \in \mathbb{R}, \qquad (1)$$

where k is a positive constant and ρ a normalized probability density. The usual Boltzmann-Gibbs-Shannon (BGS) entropy is recovered when $q = 1$ [$S_1 = -k\int \mathrm{d}x \rho(x) \ln \rho(x)$].

Many experimental and numerical data are well approximated by q-exponentials (the probability distributions that maximize S_q under simple constraints), giving indirect support to the applicability of the new entropic measure to those systems. In the case of the high-dimensional systems of interest in statistical physics, first-principle derivations are still to be made. However, Tsallis' entropy seems to be the appropriate one for certain low-dimensional dynamical systems, such as the Feigenbaum attractor (edge of chaos), where the usual Lyapunov exponent vanishes. In such case the characteristic value of q is related to relevant properties of the dynamics and it can be calculated by several paths, such as the multifractal spectrum of the attractor [3] or the sensitivity to initial conditions [4], or even, from a rigorous renormalization group analysis [5]. Furthermore, this scenario has been shown to be valid also for two-dimensional maps [6].

One of the properties of S_q that, for an appropriate value of the entropic index, can make it in some cases preferable to the standard entropy is the possibility of having an asymptotic rate of entropy production with a non-trivial value. Among the a priori infinite possible values of q, the one leading to a linear increase of the entropy with time, implying *finite* rate of entropy growth, is selected as being q_c, a value of q characteristic of the system. In fact, this is another path for the determination of q that in the case of unimodal maps [7] provides the same results as the alternative methods mentioned above. Moreover, rigorous analytical results have recently been found for such systems along this line [8]. The consistent results obtained for the edge of chaos [3–5,7,8] have encouraged the study of the temporal evolution of the S_q family (allowing to determine q_c) for diverse other dynamical systems [9–12]. The outcome $q_c \neq 1$ has usually been interpreted as a

[a] e-mail: celia@cbpf.br

signal of nonextensivity or complexity. However, we will see that this may be not always the case.

A particular system where the criterion of finite entropy rate has been applied before is the cyclic Lotka-Volterra model in a lattice (LLV) [12]. The LLV is one of the descendants of the original versions constructed by Lotka[13] and Volterra [14] to model autocatalytic chemical reactions and the prey-predator dynamics, respectively, and further adapted to many other situations from active transport by proteins [15] to social processes [16]. The generalized LLV extends the original scheme to $\mathcal{N}$ species A_i ($i = 1, \ldots, \mathcal{N}$) such that, cyclically, A_i is "predator" of A_{i-1} and simultaneously "prey" of A_{i+1} (with $A_{\mathcal{N}+1} \equiv A_1$). Furthermore, the dynamics takes place over a lattice, an ingredient that introduces new interesting spatial features in comparison to the spatially homogeneous mean-field description [17]. Its remarkable traits, such as stationary states with spatial patterns [18] and fractality [19], present it as a potential candidate for the applicability of the entropies S_q. Precisely, the possibility of extracting useful information from the S_q entropy growth motivated its study along these lines. Previous numerical studies of the LLV in one and two dimensions led to conjecture the relation $q_c = 1 - 1/D$ for arbitrary lattice dimensionality D [12]. Here we will go a step further. After testing the conjecture in higher dimensions, we will essay an interpretation of the connection between q_c and space dimensionality. We will see that $q_c \neq 1$ is not necessarily related to the fractal properties of the dynamics, contrarily to what occurs, for instance, in the logistic maps at the edge of chaos [3–5,7,8].

The remaining of the paper is organized as follows. In Section 2 we describe in detail the specific LLV model considered. In Section 3 the time behavior of the entropies S_q associated to the LLV is studied. Section 4 exhibits the behavior of S_q under simple transformations of a probability density leading to reanalyze in Section 5 the LLV dynamics. Final remarks are presented in Section 6.

2 The generalized Lotka-Volterra model in a lattice

Particles of the $\mathcal{N}$ different species A_i are localized at the sites of a D-dimensional hypercubic lattice. Reactions between particles of different species occur in bimolecular autocatalytic steps following the scheme

$$A_i + A_{i+1} \xrightarrow{k_i} 2A_{i+1}, \tag{2}$$

for $i = 1, \ldots, \mathcal{N}$, being $A_{\mathcal{N}+1} \equiv A_1$, and where $0 \leq k_i \leq 1$ are the kinetic rates. No sites are empty but one of the species could be interpreted as representing empty sites in the lattice [12,19–21]. The dynamics is implemented by means of a Monte Carlo (MC) algorithm following the details in references [12,19,20]. Basically, at every microscopic step: (i) one lattice site is randomly chosen; (ii) one of its nearest neighbors is randomly chosen; (iii) if the first site is A_i and the neighbor A_{i+1}, the first site changes to A_{i+1} with probability k_i, in accord with scheme (2), otherwise the site remains unchanged. Each MC step (MCS, our unit of time) consists in $N = L^D$ microscopic steps defined above, where L is the linear size of the lattice, so that at each MCS all sites are revisited once in average. Boundary conditions are periodic. In this paper we will deal with three species only ($\mathcal{N} = 3$) and we will focus on the symmetric case where all the kinetic rates are equal to one ($k_1 = k_2 = k_3 = 1$). Moreover, we will restrict our study to a particular mode of the dynamics, the "nucleus growth" one [12,21]. The lattice is set with all the sites filled with species A_3 and a "droplet" or nucleus represented by a sublattice of small linear size λ (i.e., $\lambda \ll L$) is introduced. The droplet contains equal amounts of particles of all the three species randomly and uniformly distributed.

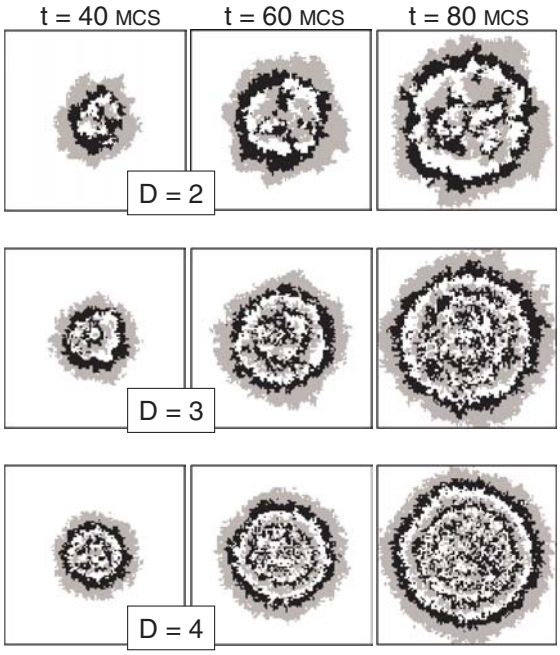

Fig. 1. Snapshots of the dynamics at different times indicated on the top of the figure, for $D = 2$, 3 and 4. The initial condition is a droplet, where all the species are present in equal amounts and homogeneously distributed, over a background of A_3. In all cases the linear size of the lattice is $L = 100$ and the initial nucleus has $\lambda = 6$. For $D > 2$ the snapshots correspond to sections parallel to one of the hypercube faces and passing by the position of the center of the initial droplet. Species are A_1 (gray), A_2 (black) and A_3 (white).

As the system evolves according to the MC dynamics, the droplet grows and acquires spontaneously a peculiar structure [22]. Typical snapshots of the dynamics are exhibited in Figure 1 for lattices in $D = 2$, 3 and 4 dimensions. Rings of alternating species develop, repeating the sequence A_1, A_2, A_3 towards the center of the droplet. This pattern is possible since all the kinetic constants are equal, then layers have almost the same radial velocity. The thickness of the rings decreases towards the center and thickness fluctuations destroy the most immersed rings. This behavior has already been observed

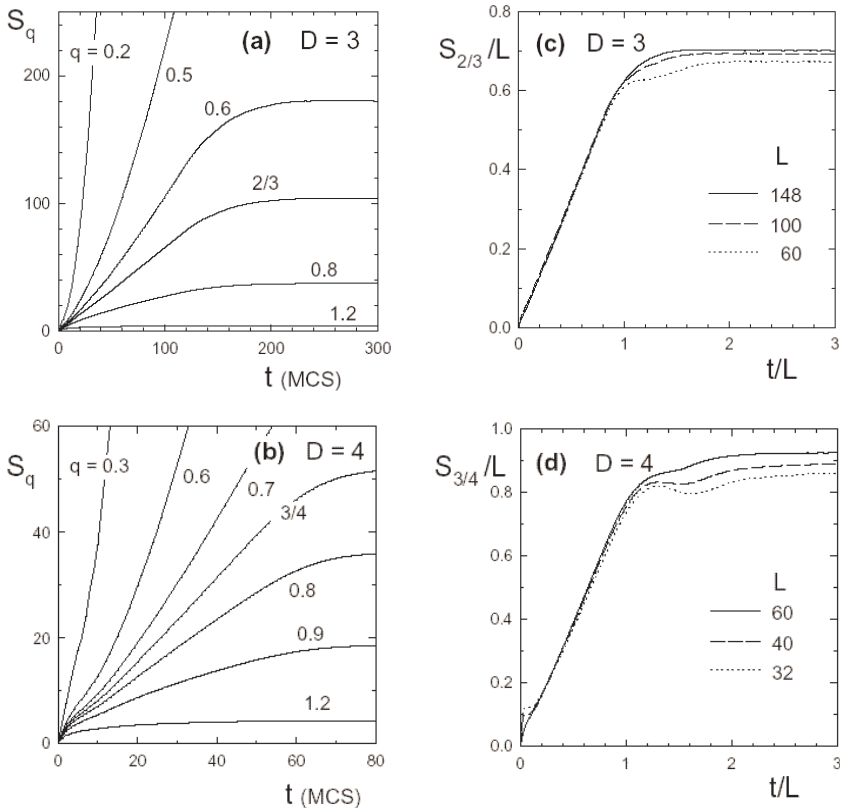

Fig. 2. Time evolution of the generalized entropies. S_q vs. t for various values of q and $L = 148$ in $D = 3$ (a), $L = 60$ in $D = 4$ (b). S_q/L vs. t/L for different lattice sizes L with: $q = 2/3$ when $D = 3$ (c), $q = 3/4$ when $D = 4$ (d). Symbols correspond to a single representative numerical experiment. In all cases, the window of the partitioning is $l = 4$ and the initial droplet size $\lambda = 4$.

before by Provata and Tsekouras for the two dimensional case [21]. They also observed that the destroyed rings give rise to a spatial organization of the species in domains with fractal boundaries typical of the steady state in fully occupied periodical lattices[12,19,21]. As the dimensionality increases, spatial features remain qualitatively similar but length scales become shorter. In the mean-field limit $D \to \infty$, homogeneity is expected. We are going to inspect immediately the evolution of spatial patterns from the viewpoint of the generalized entropies S_q.

3 Temporal evolution of S_q in the LLV

Following previous work [12], we study the temporal evolution of the entropies associated to one of the species, e.g., A_1. This particular choice does not substantially affect the results. Nonoverlapping windows or sublattices $\{W_i,\ 1 \le i \le M\}$ of edge length l covering all the lattice are considered. Thus the number of windows must be $M = (L/l)^D$, where l is a divisor of L. We associate to each window i a probability $p_i(t)$ of being occupied by species A_1 at time t by counting the number of particles of that species $n_1(i,t)$. Then $p_i(t) = n_1(i,t)/n_1(t)$, where $n_1(t)$ is the total number of particles A_1 on the lattice. The resulting set of probabilities is used to calculate the entropy of the lattice, given by the discrete version of equation (1) (where we have set $k = 1$)

$$S_q \;=\; \frac{1 - \sum_i p_i^q}{q-1}. \qquad (3)$$

The LLV in $D = 1$ and 2 dimensions has already been studied from this viewpoint before [12]. Now we will investigate higher dimensional lattices. Figure 2 shows the generalized entropies as a function of time for diverse values of q, when the lattice has $D = 3$ and 4 dimensions. The results shown in Figure 2 are not qualitatively affected by changing l and/or L, as long as $1 \le l \ll L$. They mainly affect the saturation level, that for the uniform distribution is $S_q^{sat.} = [(L/l)^{D(1-q)} - 1]/(1-q)$.

Notice in Figures 2a and b that as q increases the concavity passes from positive to negative, before saturation, which occurs when the droplet radius becomes of the order of the linear size of the lattice. Entropies with q yielding constant slope (null concavity) are represented as a function of time in Figures 2c and d. In all cases, constant slope occurs at a value of the entropic index q_c that as function of D follows the law

$$q_c \;\simeq\; 1 - \frac{1}{D}, \qquad (4)$$

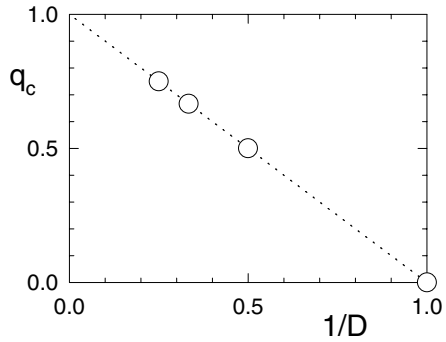

Fig. 3. Characteristic value q_c as a function of the lattice dimensionality D. The dotted straight line corresponds to $q_c = 1 - 1/D$. Symbols are the result of numerical experiments. Errors are of the order of symbol size. For $D = 3$ and 4: q_c was numerically determined from the data in Figure 2 as the value of q yielding a linear slope. For $D = 1$ and 2, q_c was extracted from reference [12].

in agreement with the relation numerically found for $D = 1$ and 2, and conjectured for generic D previously [12]. See Figure 3.

4 Behavior of S_q under simple transformations of a probability density

The characteristic entropic index q_c is related to the number of dimensions D though a simple law. This leads to think that a simple mechanism could be behind. Since we are dealing with an isotropic growth process, we will investigate in this section the relation between q_c and D resulting from some basic growth mechanisms and connect it with equation (4).

Let us analyze the behavior of the entropies S_q under a rescaling transformation of an arbitrary probability density $\rho(x)$, being x a point in a D-dimensional space [23]. The entropy of the rescaled function $\rho_\sigma(x) = \rho(x/\sigma)/\sigma^D$, where σ is a linear length, becomes

$$S_q(\sigma) \;=\; \frac{\sigma^{(1-q)D}\Big((1-q)S_q(1)+1\Big)-1}{1-q}. \qquad (5)$$

As $\sigma \to \infty$, the distribution broadens and the entropy grows due to the loss of order. If the scaling or stretching parameter increases exponentially with time, linear entropy increase occurs for $q = 1$. If the scaling parameter follows the law $\sigma \sim t^{\gamma/2}$ with $\gamma > 0$, then the generalized entropies increase with time as follows: For $q < 1$, they scale with time as $S_q(t) \sim t^{(1-q)D\gamma/2}$, $S_q(t) \sim \ln t$ in the marginal case $q = 1$, and for $q > 1$, saturation occurs at $S_q(\infty) = 1/(q-1)$. Hence a linear increase is achieved in the regime $q < 1$ for

$$q_c \;=\; 1 - \frac{2}{\gamma D}. \qquad (6)$$

As a relevant particular case let us mention the isotropic normal diffusive spreading of a D-dimensional Gaussian distribution where the stretching parameter is $\sigma^2(t) = 2Qt$, with Q the positive diffusion constant. In this case $\gamma = 1$ then $q_c = 1 - 2/D$. The general case given by equation (6) may be due to anomalous diffusive motion. A still simpler example of rescaling transformation that will be useful later consists in a density being non-null and uniform inside a D-dimensional hypersphere and zero outside, such that the radius $\sigma(t)$ grows as $\sigma \sim t^{\gamma/2}$. Notice that the expression for q_c of the growing LLV droplet, given by equation (4), is obtained when the temporal variation of the scaling length σ is ballistic ($\gamma = 2$).

Now, let us consider another simple process. $M \gg N$ windows cover a lattice, like for the LLV in the previous Section, with probabilities

$$(p_1, p_2, \ldots, p_N, \underbrace{0, 0, \ldots, 0}_{M-N}), \qquad \sum_{1\le i\le N} p_i = 1.$$

Imagine that windows with non-null probability are replicated by an integer factor m such that the new set of probabilities is

$$\Big(\underbrace{\frac{p_1}{m}, \ldots, \frac{p_1}{m}}_{m}, \underbrace{\frac{p_2}{m}, \ldots, \frac{p_2}{m}}_{m}, \ldots, \underbrace{\frac{p_N}{m}, \ldots, \frac{p_N}{m}}_{m}, \underbrace{0, 0, \ldots, 0}_{M-mN}\Big).$$

If the replication factor is $m \sim \sigma^D$ (where σ is a typical linear size of the D-dimensional system) and additionally if $\sigma \sim t^{\gamma/2}$, then the entropy will be produced in such a way that a growth linear in time occurs for q_c given by equation (6). In fact, if a continuous distribution is discretized, the associated rescaling process can be thought as a particular case of the replication one here considered, a special case where replicas are spatially ordered. Nevertheless, the entropy does not depend on the spatial localization of the windows.

Summarizing, while for an ordinary exponential growth process, the standard entropy S_1 increases linearly with t; for a process where growth follows a power-law in time, S_q has the property of finite asymptotic entropy rate for some $q = q_c \neq 1$. This value of the entropic index can result from simple transformations and therefore may be trivially related to the lattice dimensionality. These ideas lead us to review the results of the precedent section to see whether simple mechanisms are also lurking there.

5 Some details of the LLV dynamics

Let us inspect first the roughness of the interface because the reaction rate and therefore the dynamics of the propagating front are related to that quantity. Since we are interested in the interface, one can perform numerical simulations considering just two species. Hence we follow the evolution of an initial nucleus containing only A_1 particles dropped over a background of A_3. Its propagation is like in the LLV case where a forefront of A_1 particles governs the spreading of the droplet. Since the reaction rate must be proportional to the "extent" of the interface, we measure N_s, the number of reactive sites constituting the

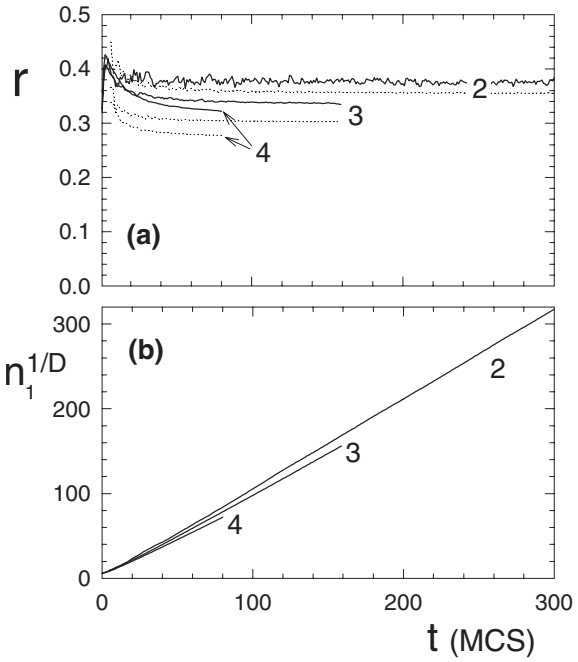

Fig. 4. Propagation of a droplet of A_1 in a lattice filled with A_3, for different values of D indicated in the figure. (a) Reactivity r as a function of time for the two-species LLV (full lines); for comparison, r for a regularly filled hypersphere with the same total number of cells as the corresponding LLV nucleus is also plotted (dotted lines). (b) Total number of sites n_1 occupied by A_1 vs. time. The initial nucleus has linear size $\lambda = 4$.

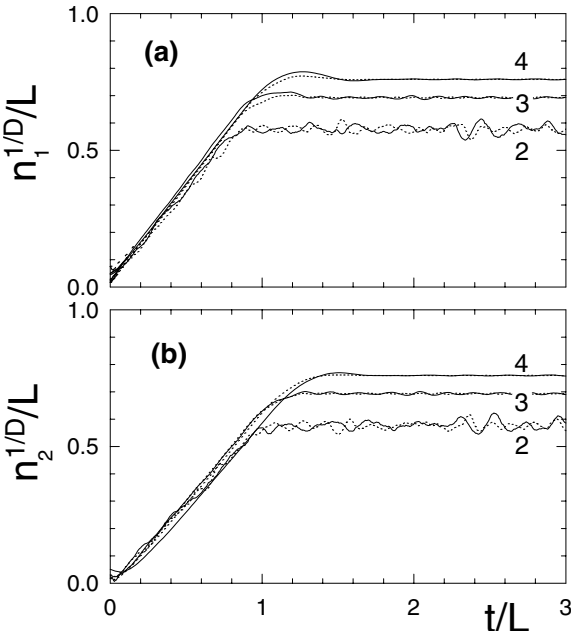

Fig. 5. Time evolution of the number of cells n_1 and n_2 occupied by species A_1 (a) and A_2 (b), respectively, for the values of the lattice dimensionality indicated in the figure and for various lattice sizes L: 150 and 200 ($D = 2$), 100 and 150 ($D = 3$), and 60 and 100 ($D = 4$), represented by dotted and full lines respectively. Time is measured in MCS. Curves correspond to single runs. The initial droplet size is $\lambda = 6$ for $D = 2$ and $\lambda = 4$ for $D = 3, 4$.

interface, and N_f, the total number of reactive faces in interfacial sites. Reactive faces are those separating two nearest neighboring sites occupied by different species. A suitable quantity for our growth process is

$$r = \frac{N_f}{cN_s}, \tag{7}$$

where c is the connectivity, i.e, the number of first nearest neighbors *per* site ($c = 2D$ in hypercubic lattices). The quantity r represents an averaged measure of the degree of reactivity of an interfacial site, and must be also connected to the roughness of the interface. The reactivity r is plotted in Figure 4a as a function of time. It soon reaches a stationary value within small fluctuations. For comparison, the figure also exhibits the value of r for a regularly filled hypersphere with the same total number of cells as in the LLV nucleus at each given t. The higher the lattice dimensionality, the larger the relative difference between the values of r for the two models. The roughness of the propagation front in the 1D dynamics has been studied in detail by Provata and Tsekouras [21]. Also in this case, it was shown that after a brief transient the rough profile remains stable in average.

If the reactivity remains constant in time, the front moves at constant radial speed: $R(t) = R(0) + v\,t$, where R is an effective radius $R \propto n_1^{1/D}$ and the velocity $v \equiv v(r)$ an increasing function of its argument for a given D. Although the fractal properties of the interface are embodied in the velocity, if the roughness soon reaches its steady value, then fractality does not affect the temporal law of the front propagation. In effect, the linear dependence of R with time is observed in numerical experiments (see Fig. 4b). Therefore, following the considerations of the precedent section, equation (6) with $\gamma = 2$ must clearly hold in this binary case.

In the three-species case, although the reaction scheme is cyclic, symmetry is broken by the initial condition. Species A_3 plays the special role of a background what in turn makes A_1 play the special role of the forefront species. After a short transient and before the limits of the lattice are reached by the nucleus, the stationarity of the interface reactivity r leads to a linear growth of the effective radius with time, as in the two species case. Consequently, the total number of cells in the nucleus, protected by the most external ring constituted by A_1 cells, will increase as t^D. Behind the first ring, the three species are equivalent, then the total number of cells occupied by each species in the nucleus is expected to increase with the same law t^D too. In fact, this behavior is observed in numerical simulations, as shown in Figure 5, although species A_1 yields a slightly larger slope than A_2. Linear growth implies a regime where the concentrations in the nucleus are conserved. When full occupation of the lattice is attained, the concentration of each species $c_i = n_i/L^D$ ($i = 1, \ldots, 3$) fluctuates around the stable center predicted by the mean-field theory: $c_i = k_i/\sum_j k_j = 1/3$, for all i [20].

We have seen that the production of the species in the nucleus is such that after a short transient their concentrations remain approximately constant. Thus, in the extreme case when windows have the size of a cell ($l = 1$), a linear increase of S_q with time occurs clearly for q given by equation (4). In fact there will be n_1 windows with non-null probability $1/n_1$, where $n_1(t) \sim t^D$, then $S_q(t) = (n_1^{1-q} - 1)/(1-q)$, so that: $S_q \sim t$, if $(1-q)D = 1$. In the opposite extreme where windows are so large that all non-empty windows have approximately the same occupation number, that same temporal dependence is obtained too.

Let us analyze what happens for intermediate window sizes. Clusters of cells of each species like in fully occupied lattices [12,19] appear in the interior of the nucleus. It is not counterintuitive the idea that as the volume of the nucleus is increasing, the size distribution of the agglomerates becomes stationary after a transient. To test this idea one can calculate for instance the occupation numbers of the windows, intimately related to entropy computation, and see how their distribution evolves in time. Figure 6 exhibits the number of windows $\Omega(i)$ occupied by at most i cells of species A_1 ($1 \leq i \leq l^D$), for different time instants. The occupation number for $i = 0$ is dismissed whereas it does not contribute to the entropy and a cumulative probability is considered in order to get smoother curves. Notice that the curves in the log-linear plot are practically parallel, indicating that they differ in a multiplicative factor. Moreover, the replication factor increases following the law t^D as illustrated in the inset of Figure 6 and in accord with previous considerations. All this means that a replication of the windows as described in Section 4 with $\gamma = 2$ is going on.

In conclusion, the analysis of both interfacial and bulk contributions to the growth process shows that, although the underlying dynamics is complex, once the properties of spatial structures attain steady values, growth is controlled by simple laws. More explicitly, the resulting growth processes are power-law in time with scaling exponents trivially related to the lattice dimensionality since $\sigma \sim t$ (corresponding to $\gamma = 2$). Then, the linear increase of S_q with time for q_c given by equation (4) is expected for arbitrary D.

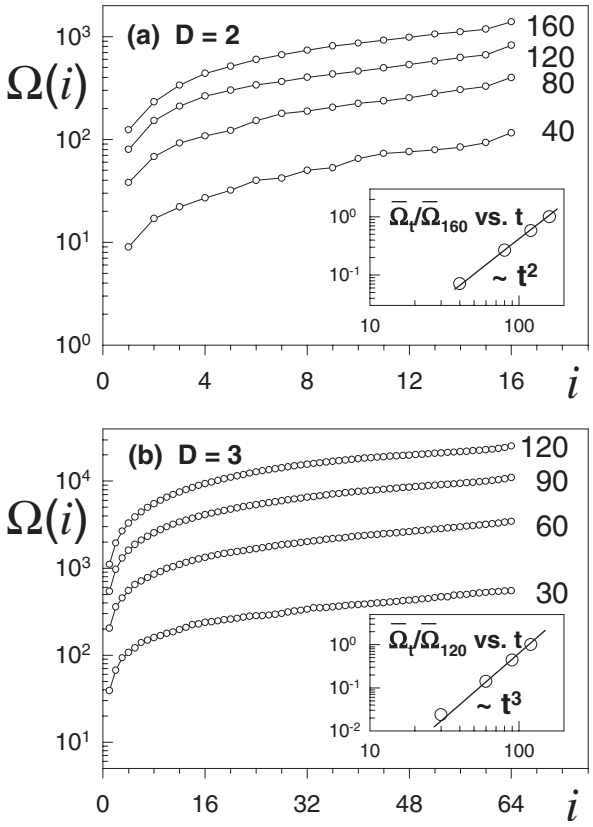

Fig. 6. Cumulative distribution of occupation numbers at different times (in MCS) indicated in the figure for $D = 2$ (a) and $D = 3$ (b). $\Omega(i)$ is the number of windows occupied by less than i cells of species A_1 ($1 \leq i \leq l^D$). In all cases, the window edges have length $l = 4$. For $D = 2$, $(L, \lambda) = (200, 6)$, and for $D = 3$, $(L, \lambda) = (148, 4)$. Insets: multiplication factor $\bar{\Omega}_t/\bar{\Omega}_{t_{max}}$ as a function of time (in MCS), where the horizontal bars mean average over all the occupation numbers at a given t, and $t_{max} = 160$ (a), 120 (b).

6 Final remarks

In this paper we have employed the criterion of finite asymptotic growth rate of S_q to determine q_c in the D-dimensional LLV. We verified for $D = 3$ and $D = 4$ a conjecture for the connection between q_c and D previously proposed [12], namely, $q_c = 1 - 1/D$. Moreover we detected the mechanisms leading to such relation for generic D.

The box-counting method applied to the 2D LLV [19] has previously shown that the boundaries of the small domains of a given species are approximately fractal [19] with a fractal dimension d_f that depends on the reaction rates k_i. Analogous results are expected in higher dimensions. We have seen that, for the present model and for the particular probability assignment considered, S_q entropy production does not capture directly the fractality of spatial patterns. Of course, since the fractal dimension d_f must depend on the lattice spatial dimension D, the characteristic entropic index q_c (a function of D) results in some way connected to d_f. But q_c is not determined by the degree of fractality, it is only determined by D, independently of the nature (fractal or not) of the growing core. This is so because the properties of spatial patterns, such as the interface roughness, soon reach steady values.

In a process where the number of occupied cells increases exponentially with time t, the usual BGS entropy S_1 increases linearly with t. For a growth process that is not exponential, one can not expect a linear increase of the standard entropy S_1. Particularly, if growth occurs following a power-law in time, S_q has the property of finite production rate for some $q = q_c \neq 1$, as shown in Section 4. Then $q_c \neq 1$ is the expected outcome, not necessarily connected to the complex features of a system. This is what we observe in the present study where q_c is trivially related to the lattice dimensionality and, therefore,

it does not furnish significant information on the dynamics. However, q_c may be non-trivial in other instances. An example is the Feigenbaum attractor, cited in the Introduction. In that case, a suitably chosen small segment σ of initial conditions grows following the law $\sigma \sim t^{\gamma/2}$ (sensitivity to initial conditions), where $\gamma \equiv 2/(1-q_c)$ with $q_c = 0.2445\ldots$ [8], yielding a finite rate of S_{q_c}, in accord with the considerations made in Section 4. The entropic index q_c was shown to be a relevant quantity related to the geometry of the multifractal attractor [3].

We have seen that the stationarity of certain properties of the LLV dynamics determines a growth process linear in time ($\gamma = 2$), yielding relation (4). As perspectives, one can not exclude the possibility that in other dynamical regimes of the LLV, the increase of S_q can reflect complex features. Also, it could be insightful to review previous works in the literature by taking into consideration the present results. This might be especially fruitful in cases where characteristic indexes of the form $q_c = 1 - 2/(\gamma D)$ have also been found, as in the interesting study of Galilean-invariant lattice Boltzmann models of fluids [11].

I am very grateful to Fulvio Baldovin and Constantino Tsallis for interesting and fruitful discussions. I also thank Astero Provata for useful comments on the LLV. This work was partially supported by Brazilian agencies FAPERJ and PRONEX.

References

1. C. Tsallis, J. Stat. Phys. **52**, 479 (1988)
2. *Non-extensive Statistical Mechanics and Thermodynamics*, edited by S.R.A. Salinas, C. Tsallis, Braz. J. Phys. **29** (1999); *Non-extensive Statistical Mechanics and its Applications*, edited by S. Abe, Y. Okamoto, Lecture Notes in Physics, Vol. 560 (Springer-Verlag, Heidelberg, 2001); *Non-extensive Thermodynamics and Physical Applications*, edited by G. Kaniadakis, M. Lissia, A. Rapisarda [Physica A **305** (2002)]; *Anomalous Distributions, Nonlinear Dynamics and Non-extensivity*, edited by H.L. Swinney, C. Tsallis [Physica D (2004)], in press; *Non-extensive Entropy – Interdisciplinary Applications*, edited by M. Gell-Mann, C. Tsallis (Oxford University Press, New York, 2004)
3. M.L. Lyra, C. Tsallis, Phys. Rev. Lett. **80**, 53 (1998)
4. C. Tsallis, A.R. Plastino, W.-M. Zheng, Chaos Solitons Fractals **8**, 885 (1997); U.M.S. Costa, M.L. Lyra, A.R. Plastino, C. Tsallis, Phys. Rev. E **56**, 245 (1997)
5. F. Baldovin, A. Robledo, Phys. Rev. E **66**, 045104 (2002); F. Baldovin, A. Robledo, Europhys. Lett. **60**, 518 (2002)
6. U. Tirnakli, Phys. Rev. E **66**, 066212 (2002)
7. V. Latora, M. Baranger, A. Rapisarda, C. Tsallis, Phys. Lett. A **273** 97 (2000); M. Baranger, V. Latora, A. Rapisarda, Chaos, Solitons and Fractals **13**, 471 (2002)
8. F. Baldovin, A. Robledo, Phys. Rev. E **69**, 045202 (2004)
9. U. Tirnakli, G.F.J. Ananos, C. Tsallis, Phys. Lett. A **289**, 51 (2001)
10. N. Lemke, R.M.C. de Almeida, Physica A **325**, 396 (2003)
11. B.M. Boghosian, P.J. Love, P.V. Coveney, I.V. Karlin, S. Succi, J. Yepez, Phys. Rev. E **68** 025103 (2003)
12. G.A. Tsekouras, A. Provata, C. Tsallis, Phys. Rev. E **69**, 016120 (2004)
13. A.J. Lotka, Proc. Natl. Acad. Sci. U.S.A. **6**, 410 (1920)
14. V. Volterra, *Leçons sur la théorie mathématique de la lutte pour la vie* (Gauthier-Villars, Paris, 1931)
15. F.M.C. Vieira, P.M. Bisch, Physica A **199**, 40 (1993)
16. J.M. Epstein, *Nonlinear dynamics, mathematical biology, and social science* (Addison-Wesley, Don Mills-Ontario, 1997)
17. L. Frachebourg, P.L. Krapivsky, E. Ben-Naim, Phys. Rev. E **54**, 6186 (1996)
18. K.-I. Tainaka, Phys. Rev. Lett. **63**, 2688 (1989)
19. G.A. Tsekouras, A. Provata, Phys. Rev. E **65**, 016204 (2002)
20. A. Provata, G. Nicolis, F. Baras, J. Chem. Phys. **110**, 8361 (1999)
21. A. Provata, G.A. Tsekouras, Phys. Rev. E **67**, 056602 (2003)
22. Occasionally, if the initial droplet is too small, it may be invaded by one of the species
23. C. Anteneodo, A.R. Plastino, Phys. Lett. A **223**, 348 (1996)